White Rose Research Online

eprints@whiterose.ac.uk
https://eprints.whiterose.ac.uk
Universities of Leeds, Sheffield and York

Deposited via The University of Sheffield.

White Rose Research Online URL for this paper:
https://eprints.whiterose.ac.uk/id/eprint/139127/

Version: Published Version

Article:
Foster, A.P., Hallett, D., Iorsh, I.V. et al. (2019) Tunable photon statistics exploiting the Fano effect in a waveguide. Physical Review Letters, 122 (17). 173603. ISSN: 0031-9007

https://doi.org/10.1103/PhysRevLett.122.173603

© 2019 American Physical Society. Reproduced in accordance with the publisher's self-archiving policy.

Reuse
Items deposited in White Rose Research Online are protected by copyright, with all rights reserved unless indicated otherwise. They may be downloaded and/or printed for private study, or other acts as permitted by national copyright laws. The publisher or other rights holders may allow further reproduction and re-use of the full text version. This is indicated by the licence information on the White Rose Research Online record for the item.

Takedown
If you consider content in White Rose Research Online to be in breach of UK law, please notify us by emailing eprints@whiterose.ac.uk including the URL of the record and the reason for the withdrawal request.

UNIVERSITY OF LEEDS
University of Sheffield
UNIVERSITY of York

Tunable Photon Statistics Exploiting the Fano Effect in a Waveguide

A. P. Foster,[1,*] D. Hallett,[1] I. V. Iorsh,[2] S. J. Sheldon,[1] M. R. Godsland,[1] B. Royall,[1] E. Clarke,[3] I. A. Shelykh,[2,4] A. M. Fox,[1] M. S. Skolnick,[1,2] I. E. Itskevich,[5] and L. R. Wilson[1,†]

[1]*Department of Physics and Astronomy, University of Sheffield, Sheffield S3 7RH, United Kingdom*
[2]*ITMO University, St. Petersburg 197101, Russia*
[3]*EPSRC National Epitaxy Facility, University of Sheffield, Sheffield S1 3JD, United Kingdom*
[4]*Science Institute, University of Iceland, Dunhagi 3, IS-107 Reykjavik, Iceland*
[5]*Department of Engineering, University of Hull, Hull HU6 7RX, United Kingdom*

(Received 22 November 2018; published 3 May 2019)

A strong optical nonlinearity arises when coherent light is scattered by a semiconductor quantum dot coupled to a nanophotonic waveguide. We exploit the Fano effect in such a waveguide to control the phase of the quantum interference underpinning the nonlinearity, experimentally demonstrating a tunable quantum optical filter which converts a coherent input state into either a bunched or an antibunched nonclassical output state. We show theoretically that the generation of nonclassical light is predicated on the formation of a two-photon bound state due to the interaction of the input coherent state with the quantum dot. Our model demonstrates that the tunable photon statistics arise from the dependence of the sign of two-photon interference (either constructive or destructive) on the detuning of the input relative to the Fano resonance.

DOI: 10.1103/PhysRevLett.122.173603

The generation of nonclassical light is a fundamental requirement for the operation of quantum photonic devices. For instance, a single photon input is a prerequisite for linear optical quantum computation schemes [1], while the use of entangled photon states may enable sensing with Heisenberg-limited precision in the field of quantum metrology [2,3]. On-demand, single-photon emitters such as quantum dots (QDs) are a proven resource for nonclassical light, enabling the generation of single- [4,5] and two-photon [6] states, as well as the creation of entangled states on chip [7].

A markedly different approach to generate nonclassical light (and to tune the photon statistics in general) involves the manipulation of a coherent input state, in such a way that the output state becomes either bunched or antibunched. A coherent input state can be considered as a weighted sum of different number states [8]. Number-state filtering, in which the weighting of the individual number states is controlled, can generate a quantum output state from such a classical coherent input (for instance, via photon blockade [9–13]). The use of interference has emerged as an extremely powerful tool in this regard: it has been shown theoretically that it can be used to realize complex photon statistics in cavity [14–16] and waveguide [17,18] quantum electrodynamics (QED), and to generate single photons with simultaneous subnatural linewidth using resonance fluorescence [19]. Experimentally, the photon statistics of a coherent input have been manipulated via quantum interference in the weakly coupled regime of cavity QED [20,21], most recently using the unconventional photon blockade [22].

An example of an interference phenomenon widely observed in photonics is the Fano effect [23]. A Fano resonance arises due to interference between a discrete transition and a background continuum, with the maxima and minima of the resulting spectral line shape arising from constructive and destructive interference, respectively. It has been shown theoretically that the detuning relative to the Fano resonance can be used to enable tunable number-state filtering [17,24,25]. To demonstrate this, we employ an integrated quantum photonic device comprising a single quantum two-level system, namely a QD, coupled to a single-mode optical waveguide. An ideal waveguide (with 100% transmission) supports a background continuum of modes which have constant phase. Single photons resonant with the QD transition would be fully reflected due to destructive interference in the transmission direction between the continuum and photons scattered by the QD [26]. This would result in a symmetric spectral profile in transmission, as shown in Fig. 1(a). However, in a real device, reflections within the waveguide [see schematic in Fig. 1(b)] can lead to the formation of Fabry-Pérot (FP) modes, which modulate the transmission and hence the phase of the continuum. The spectral line shape in transmission then depends on the detuning of the QD transition relative to the FP modes, as shown in Fig. 1(b). In particular, when the QD transition is detuned from a mode maximum, a characteristic Fano line shape is observed [27,28].

 © 2019 American Physical Society

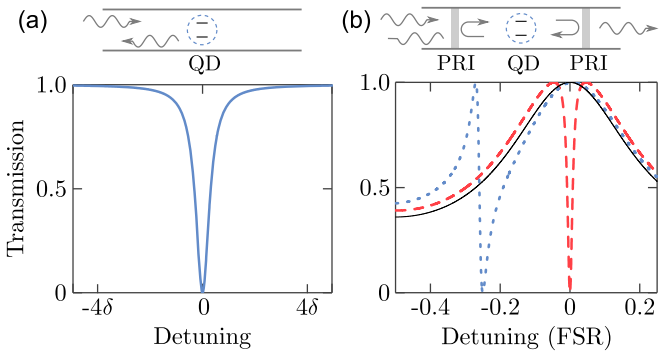

FIG. 1. (a) Calculated single-photon transmission for a waveguide containing a single QD (upper schematic), as a function of the input detuning relative to the QD transition. δ is the QD transition linewidth. (b) Calculated transmission for a waveguide containing a single QD and supporting FP modes due to partially reflective interfaces (PRIs) in the waveguide (upper schematic). The QD transition is either resonant (dashed red line) or nonresonant (dotted blue line) with the FP mode. The transmission for the same waveguide without a QD is shown by a black solid line for reference. FSR stands for free spectral range.

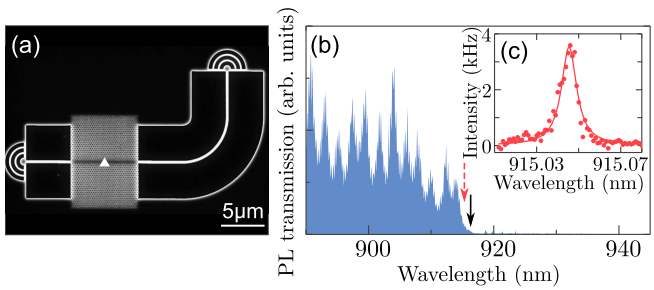

FIG. 2. (a) Scanning electron microscope image of the nanophotonic device. The triangle shows the approximate location of the QD studied here, situated in a slow light PCWG. (b) Device transmission probed using high power nonresonant PL (500 μW at 780 nm). The black arrow indicates the location of the photonic band edge. (c) Resonant photoluminescence excitation spectrum for the trion state of the QD located in the PCWG (circles), with spectral position given by the red dashed arrow in (b). The background laser scatter has been subtracted. The line is a Voigt fit to the data.

For the output photon statistics of such a device, the behavior of two-photon states is of importance. It has been predicted for an ideal waveguide that, on resonance with the discrete transition, two-photon states are preferentially transmitted (a manifestation of the nonlinear interaction between photons and the emitter at the single- or few-photon level), and the output state is bunched [26]. Similarly, bunching will occur when the input is detuned to the destructive interference regime of a Fano resonance. Notably, however, when the input is detuned to the constructive interference regime, the possibility arises of the output state being antibunched [25]. Such a nonclassical output state, tunable across the Fano resonance, has yet to be demonstrated for an integrated quantum photonic device.

In this Letter, we demonstrate a tunable quantum optical filter using an integrated device comprising a single QD coupled to a single-mode nanophotonic waveguide. We inject a tunable, coherent laser field into the waveguide, and observe a Fano resonance in transmission. We show that the transmitted state photon statistics are antibunched when resonant with the Fano maximum and bunched at the Fano minimum, evidence of tunable number-state filtering. The tuning can be achieved either by changing the laser wavelength or by electrically Stark shifting the QD transition, demonstrating control of the photon statistics locally, on chip. We model the system and show that the formation of a two-photon bound (frequency entangled) state is critical to observe number-state filtering. Furthermore, antibunching is only achieved in the case of destructive interference of two-photon product states and bound states, which becomes possible due to the Fano resonance.

Figure 2(a) shows a scanning electron microscope image of our quantum optical filter, which was fabricated within a 170-nm-thick, GaAs *p-i-n* membrane. InGaAs self-assembled QDs were embedded in the intrinsic region of the membrane and could be Stark tuned by application of a bias to the diode. (Details of the wafer, device design, and experimental procedures can be found in the Supplemental Material [29].) The device consists of a suspended single-mode photonic crystal waveguide (PCWG) with nanobeam waveguides attached to either end. The waveguides are terminated with semicircular Bragg gratings which enable vertical in- and out-coupling of light. The PCWG has a photonic band edge at ~916 nm, which was measured using waveguide-transmitted, nonresonant photoluminescence (PL) from the ensemble of QDs. The PL was excited in one Bragg coupler and detected from the other coupler, and is shown in Fig. 2(b). FP modes are revealed through oscillations in the transmitted intensity. The mode spacing of ~2 nm suggests that the dominant reflection occurs at the two Bragg coupler-nanobeam waveguide interfaces.

QDs emitting in spectral proximity to the PCWG band edge experience a slow light-induced Purcell enhancement [31]. The Purcell enhancement increases the QD exciton decay rate and consequently reduces the impact of dephasing on the coherence of the exciton emission. It also increases the β factor which characterizes the optical coupling strength between the QD and the waveguide mode [32], with a value as large as 0.98 previously reported [33]. In this regime, the QD may be considered as a "1D atom," coupling almost uniquely to the single mode of the waveguide.

Resonance fluorescence measurements, with excitation from above the QD and collection from an out-coupler, were used to locate a suitable single QD in the PCWG. Figure 2(c) shows the resonant photoluminescence

excitation spectrum for such a QD, obtained by scanning a narrow band continuous wave laser across the QD transition. Its wavelength of 915.045 nm lies within 1 nm of the PCWG band edge. The transition is likely to be a charged trion, as we typically observe fine-structure splitting for the QD neutral exciton in this sample [34]. In a separate measurement using resonant pulsed excitation (not shown), the lifetime of the trion state was found to be 150 ± 30 ps, which corresponds to a radiatively limited linewidth of 4–6 μeV. We measured an ensemble lifetime of 750 ps for QDs in the bulk of the sample and therefore estimate a Purcell factor of ~5. The linewidth in Fig. 2(c) is broadened to 15 μeV due to spectral wandering. We note that the QD could be Stark tuned over more than 100 μeV, enabling full electrical control of the laser-trion detuning.

We next probe the effect of the same single QD on the waveguide transmission. A weak, tunable, continuous-wave laser was injected into the waveguide. The laser power was chosen such that, on average, less than one photon interacted with the QD within the trion lifetime. The transmission is therefore largely determined by the interaction of single photons with the QD. Figure 3(a) shows the transmission as a function of laser-trion detuning, which was controlled by changing the laser wavelength [29]. The transmission is normalized to the background level measured in the absence of the laser-trion interaction. (This was achieved by electrical tuning of the QD transition far out of resonance with the laser.) A characteristic dispersive Fano line shape is observed, due to interference between photons scattered from the QD and the driving laser field. Note that the minimum transmission is as small as 40%, which is evidence for the strong interaction between single photons and the QD.

Now we consider the photon statistics of the transmitted field. Using a Hanbury Brown–Twiss setup, the second order autocorrelation function $g^{(2)}(\tau)$ was measured as a function of laser-trion detuning. The convolved instrument response time was 80 ps. In Figs. 3(b) and 3(c) we compare the normalized $g^{(2)}(\tau)$ histograms for laser-trion detunings of $+9$ and -9 μeV, which correspond to the Fano transmission minimum and maximum, respectively. At a detuning of $+9$ μeV substantial bunching is observed, with $g^{(2)}(0) = 2.02 \pm 0.07$. After deconvolution with the instrument response function, we obtain a $g^{(2)}(0)$ value of 2.20 ± 0.08, which is greater than the thermal classical limit. In sharp contrast, clear antibunching is measured at a detuning of -9 μeV, demonstrating the successful filtering out of two-photon states from the coherent input state. To demonstrate the tunability of our device, Fig. 3(d) shows the measured $g^{(2)}(0)$ as a function of the laser-trion detuning, covering the full spectral width of the Fano resonance. From negative to positive detuning, a dispersive line shape is seen in the photon statistics, while at large detuning the photon statistics are those of a coherent state, with $g^{(2)}(0)$ equal to unity. Thus, we have demonstrated that the photon statistics can be manipulated by means of number-state filtering using the detuning as the single control parameter. (See the Supplemental Material for measurements where the Stark shift of the QD transition was used as the control parameter [29].)

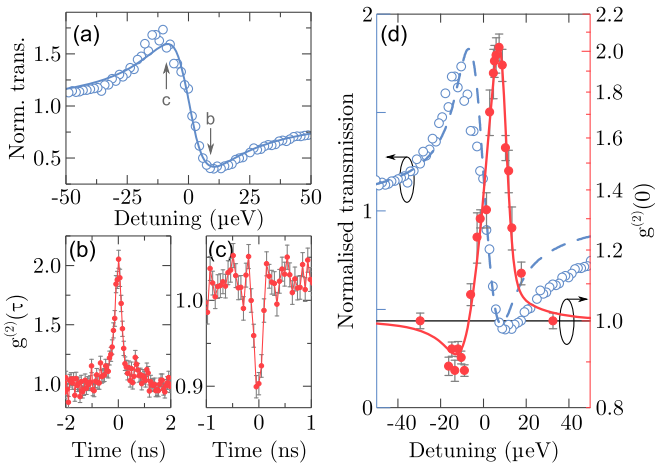

FIG. 3. (a) Measured waveguide transmission as a function of laser-trion detuning (circles), normalized to the transmission measured at large detuning. The solid line is a Breit-Wigner-Fano fit to the data. (b),(c) Second order autocorrelation function $g^{(2)}(\tau)$ at a detuning of (b) $+9$ μeV and (c) -9 μeV, as indicated in (a). The data have been normalized to the value of $g^{(2)}(\tau)$ at long time delay. Error bars correspond to the square root of the coincidence counts in each time bin. (d) $g^{(2)}(0)$ (red filled circles) and normalized waveguide transmission (blue open circles) as a function of laser-trion detuning. Error bars originate from fitting of the full $g^{(2)}(\tau)$ data. Solid and dashed lines represent the result of modeling (see text for details). The axis for $g^{(2)}(0)$ is logarithmic.

Understanding of the output photon statistics requires consideration of two kinds of two-photon states, namely (separable) product states and (frequency entangled) bound states [35–37]. We note that for two-photon product states, constructive or destructive interference at the Fano resonance follows that of single-photon states. This implies that in the absence of bound states, a coherent input would always result in a coherent output. Observation of photon number-state filtering must therefore be related to the formation of the bound states. Indeed, the bound states have been shown to explain bunching [37]. However, their presence alone is insufficient to explain the observed antibunching. To account for the antibunching, it is also necessary to consider interference between two-photon product states and bound states, as our following analysis shows. In particular, we identify the conditions under which antibunching becomes possible, and the role of FP modes in this.

To gain the necessary insight, we model the system using the input-output formalism [25]. The $g^{(1)}$ and $g^{(2)}$ two-time correlation functions are given by

$$g^{(1)}(t,t') = \frac{1}{t_0^2}\langle\alpha|\hat{c}_{\mathrm{out}}^{\dagger}(t')\hat{c}_{\mathrm{out}}(t)|\alpha\rangle, \qquad (1)$$

$$g^{(2)}(t,t') = \frac{\langle\alpha|\hat{c}^{\dagger}_{\rm out}(t)\hat{c}^{\dagger}_{\rm out}(t')\hat{c}_{\rm out}(t')\hat{c}_{\rm out}(t)|\alpha\rangle}{g^{(1)}(t,t)g^{(1)}(t',t')}, \quad (2)$$

where t_0 is the bare waveguide transmission amplitude in the absence of the QD, evaluated at the wavelength of the QD transition. The input coherent state is $|\alpha\rangle$, while $\hat{c}_{\rm out}$ are the output field annihilation operators. In the low power, stationary limit ($t \to \infty$), with $\beta = 1$ and neglecting QD dephasing, we find that

$$g^{(1)} = \frac{(\tilde{\delta} + \tan\phi)^2}{(1+\tilde{\delta}^2)} = |t_1|^2, \quad (3)$$

$$g^{(2)}(0) = \frac{1}{|t_1|^4}\left| t_1 t_1 + \frac{e^{2i\phi}}{T_0(1+\tilde{\delta}^2)}\right|^2 \quad (4)$$

$$= 1 + \frac{1}{T_0^2[\tilde{\delta} + \tan(\phi)]^4} + \frac{2\cos 2\phi}{T_0[\tilde{\delta} + \tan(\phi)]^2}, \quad (5)$$

where $\tilde{\delta}$ is the detuning of the laser from the QD transition. The detuning is normalized to $\gamma/2$, where γ denotes the transition decay rate. The single-photon transmission amplitude is given by t_1, $T_0 = t_0^2$, and $\phi = \tan^{-1}(-\sqrt{1-t_0^2}/t_0)$. Note that ϕ is related to the detuning of the QD transition from the FP modes. The full time-dependent expressions, also accounting for QD dephasing and nonunity β factor, can be found in the Supplemental Material [29]. We note that in the limit of a weak pump, the expression for $g^{(2)}(0)$ can alternatively be derived by the scattering matrix (S matrix) method [25,38]. Namely, in Ref. [25] an equation analogous to Eq. (4) has been derived, where the first term comes from the disconnected S matrix corresponding to the product state and the second term from the connected S matrix corresponding to the bound two-photon state.

We fit the model to the experimental $g^{(2)}(0)$ data, then use the same best-fit parameters to evaluate the normalized transmission using the equation for $g^{(1)}$. The resulting fits are shown in Fig. 3(d), showing very good agreement with the experimental results for both the transmission and the $g^{(2)}(0)$. The model clearly reproduces the most significant feature of the measured data, namely the generation of an antibunched transmitted field at negative detuning in addition to bunching at positive detuning. (See the Supplemental Material for more details of the fitting procedure [29].)

We now consider the physical process underpinning the quantum optical filter, using Eqs. (4) and (5). Equation (4) reveals interference between two-photon product states and two-photon bound states [25] (the first and the second term in the modulus squared, respectively). The first two terms in Eq. (5), obtained after evaluation of the modulus, represent the bare contributions to $g^{(2)}(0)$ from the product states (the unity term) and the bound states, respectively, and the third term describes interference between the two-photon states. Analysis of Eqs. (4) and (5) leads to several immediate conclusions. First, it is clear that the formation of the bound state is critical for the generation of nonclassical light, as in its absence $g^{(2)}(0)$ equals unity. Second, the bound state term in Eq. (5) is positively valued, and the first two terms combined would only lead to $g^{(2)}(0) \geq 1$, i.e., either a coherent or bunched output state. Evidently, antibunching can only arise in the case of destructive two-photon interference, for which the third term in Eq. (5) is negative. The latter is possible in the case when $\phi < -\pi/4$ and hence for bare waveguide transmission $T_0 < 0.5$. One should note that access to this regime in an otherwise ideal waveguide is enabled by the presence of FP modes (whose presence also gives rise to the Fano effect).

This is illustrated in Fig. 4, in which we plot the transmission $|t_1|^2 = g^{(1)}$ and $g^{(2)}(0)$, for representative values of $T_0 = 1$ and $T_0 = 0.15$. $T_0 = 1$ corresponds to a QD in a perfectly transmissive waveguide, while at $T_0 = 0.15$ a QD is significantly off resonant with a FP mode. When $T_0 = 1$, both the bound state contribution and the interference term are positive, and bunching is predicted across the whole range of detuning in Fig. 4(a), in agreement with Ref. [25]. However, for $T_0 = 0.15$, the interference term is negative, and where it outweighs the contribution from the bound state, antibunching occurs.

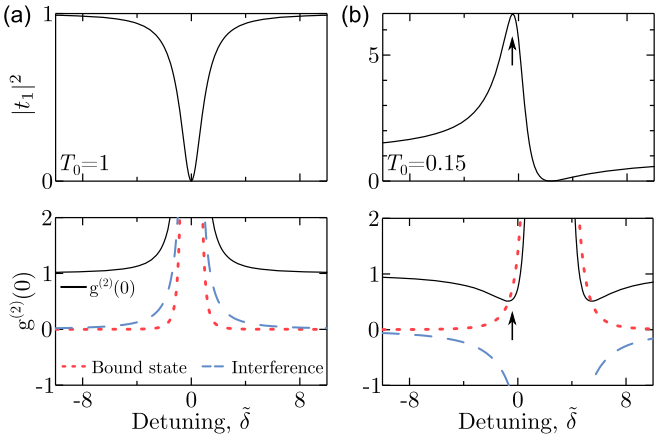

FIG. 4. Theoretical transmission $|t_1|^2$ (upper panels) and $g^{(2)}(0)$ (lower panels) (solid black lines) as a function of the detuning between the laser and the QD transition, for a bare waveguide transmission of (a) $T_0 = 1$ and (b) $T_0 = 0.15$. Antibunching can clearly be seen at a detuning corresponding to the Fano maximum, indicated by the arrows. Also shown are the contributions to the $g^{(2)}(0)$ from the two-photon bound state (red dotted lines) and the interference between two-photon product and bound states (blue dashed lines). The contribution to $g^{(2)}(0)$ from the two-photon product state is equal to unity for all detunings [see Eq. (4)].

Notably, one expects antibunching at the Fano transmission maximum, as observed experimentally. [This is indicated by arrows in Fig. 4(b).] In particular, for $T_0 = 0.15$, $g^{(2)}(0)$ is expected to be as low as 0.5 at the Fano maximum; furthermore, $g^{(2)}(0) \to 0$ as $T_0 \to 0$ in the ideal case scenario. Physically, the Fano maximum favors transmission of single photons from the coherent input. At the same time, the contribution to the output from the two-photon product states is suppressed due to destructive interference with the bound states, resulting in antibunching.

The tunable number-state filtering effect, which we observe, is therefore critically dependent on two factors: the formation of a two-photon bound state, which enables nonclassical light to be generated in the first instance, and the destructive interference of the two-photon product state and bound state. The filter switches the output between bunched and antibunched, dependent on the strength of the destructive interference effect; this in turn depends on the detuning relative to the Fano resonance.

In conclusion, we have demonstrated an integrated, tunable quantum optical filter which exploits the Fano effect to convert a coherent input state into either a bunched or antibunched nonclassical output state and provided its theoretical analysis. The filter is formed from a single QD coupled to a nanophotonic waveguide, which supports Fabry-Pérot modes. A Fano resonance is observed in the waveguide transmission as a coherent input laser is tuned across the QD transition. Antibunching of the output state is observed when the laser is resonant with the Fano maximum, and bunching at the Fano minimum. Switching between the two states is achieved by controlling the detuning of the laser relative to the Fano resonance, either by changing the laser wavelength, or locally, using the quantum-confined Stark effect. Notably, antibunching is only observed due to the presence of the Fano resonance. We have shown theoretically that the nonclassical output state is critically dependent on the formation of a two-photon bound state due to interaction of the coherent input with the QD, and that control over the photon statistics arises due to the change between constructive and destructive two-photon interference at the extrema of the Fano resonance. Our results offer a new direction for the use of quantum interference effects in integrated photonic circuits; in particular, the Fano resonance is of significant interest for applications requiring fast optical switching [23,39], and our work extends this capability to switching of photon statistics.

Data supporting this study are openly available from the University of Sheffield repository [40].

This work was supported by EPSRC Grant No. EP/N031776/1 and by Megagrant 14.Y26.31.0015 of the Russian Federation. I. V. I. thanks D. Kornovan for valuable discussions.

*andrew.foster@sheffield.ac.uk
†luke.wilson@sheffield.ac.uk

[1] P. Kok, W. J. Munro, K. Nemoto, T. C. Ralph, J. P. Dowling, and G. J. Milburn, Rev. Mod. Phys. **79**, 135 (2007).
[2] M. Müller, H. Vural, C. Schneider, A. Rastelli, O. G. Schmidt, S. Höfling, and P. Michler, Phys. Rev. Lett. **118**, 257402 (2017).
[3] A. J. Bennett, J. P. Lee, D. J. P. Ellis, T. Meany, E. Murray, F. F. Floether, J. P. Griffths, I. Farrer, D. A. Ritchie, and A. J. Shields, Sci. Adv. **2**, e1501256 (2016).
[4] N. Somaschi, V. Giesz, L. De Santis, J. C. Loredo, M. P. Almeida, G. Hornecker, S. L. Portalupi, T. Grange, C. Antón, J. Demory, C. Gómez, I. Sagnes, N. D. Lanzillotti-Kimura, A. Lemaítre, A. Auffeves, A. G. White, L. Lanco, and P. Senellart, Nat. Photonics **10**, 340 (2016).
[5] X. Ding, Y. He, Z.-C. Duan, N. Gregersen, M.-C. Chen, S. Unsleber, S. Maier, C. Schneider, M. Kamp, S. Höfling, C.-Y. Lu, and J.-W. Pan, Phys. Rev. Lett. **116**, 020401 (2016).
[6] T. Heindel, A. Thoma, M. von Helversen, M. Schmidt, A. Schlehahn, M. Gschrey, P. Schnauber, J.-H. Schulze, A. Strittmatter, J. Beyer, S. Rodt, A. Carmele, A. Knorr, and S. Reitzenstein, Nat. Commun. **8**, 14870 (2017).
[7] R. J. Young, R. M. Stevenson, P. Atkinson, K. Cooper, D. A. Ritchie, and A. J. Shields, New J. Phys. **8**, 29 (2006).
[8] M. Fox, *Quantum Optics: An Introduction* (Oxford University Press, New York, 2006).
[9] A. Faraon, I. Fushman, D. Englund, N. Stoltz, P. Petroff, and J. Vuckovic, Nat. Phys. **4**, 859 (2008).
[10] A. Reinhard, T. Volz, M. Winger, A. Badolato, K. J. Hennessy, E. L. Hu, and A. Imamoğlu, Nat. Photonics **6**, 93 (2012).
[11] K. Müller, A. Rundquist, K. A. Fischer, T. Sarmiento, K. G. Lagoudakis, Y. A. Kelaita, C. Sánchez Muñoz, E. del Valle, F. P. Laussy, and J. Vučković, Phys. Rev. Lett. **114**, 233601 (2015).
[12] M. Radulaski, K. A. Fischer, K. G. Lagoudakis, J. L. Zhang, and J. Vučković, Phys. Rev. A **96**, 011801(R) (2017).
[13] H. Flayac and V. Savona, Phys. Rev. A **96**, 053810 (2017).
[14] M. Bamba, A. Imamoğlu, I. Carusotto, and C. Ciuti, Phys. Rev. A **83**, 021802(R) (2011).
[15] M. Radulaski, K. A. Fischer, and J. Vučković, Adv. At., Mol., Opt. Phys. **66**, 111 (2017).
[16] A. Majumdar, M. Bajcsy, A. Rundquist, and J. Vučković, Phys. Rev. Lett. **108**, 183601 (2012).
[17] K. A. Fischer, Y. A. Kelaita, N. V. Sapra, C. Dory, K. G. Lagoudakis, K. Müller, and J. Vučković, Phys. Rev. Applied **7**, 044002 (2017).
[18] X. H. H. Zhang and H. U. Baranger, Phys. Rev. A **97**, 023813 (2018).
[19] J. C. L. Carreño, E. Z. Casalengua, F. P. Laussy, and E. del Valle, Quantum Sci. Technol. **3**, 045001 (2018).
[20] A. J. Bennett, J. P. Lee, D. J. P. Ellis, I. Farrer, D. A. Ritchie, and A. J. Shields, Nat. Nanotechnol. **11**, 857 (2016).
[21] L. De Santis, C. Antón, B. Reznychenko, N. Somaschi, G. Coppola, J. Senellart, C. Gómez, A. Lemaître, I. Sagnes, A. G. White, L. Lanco, A. Auffèves, and P. Senellart, Nat. Nanotechnol. **12**, 663 (2017).

[22] H. J. Snijders, J. A. Frey, J. Norman, H. Flayac, V. Savona, A. C. Gossard, J. E. Bowers, M. P. van Exter, D. Bouwmeester, and W. Löffler, Phys. Rev. Lett. **121**, 043601 (2018).
[23] M. F. Limonov, M. V. Rybin, A. N. Poddubny, and Y. S. Kivshar, Nat. Photonics **11**, 543 (2017).
[24] A. Ridolfo, O. Di Stefano, N. Fina, R. Saija, and S. Savasta, Phys. Rev. Lett. **105**, 263601 (2010).
[25] S. Xu and S. Fan, Phys. Rev. A **94**, 043826 (2016).
[26] D. E. Chang, A. S. Sørensen, E. A. Demler, and M. D. Lukin, Nat. Phys. **3**, 807 (2007).
[27] A. Javadi, I. Söllner, M. Arcari, S. L. Hansen, L. Midolo, S. Mahmoodian, G. Kirsanske, T. Pregnolato, E. H. Lee, J. D. Song, S. Stobbe, and P. Lodahl, Nat. Commun. **6**, 8655 (2015).
[28] D. L. Hurst, D. M. Price, C. Bentham, M. N. Makhonin, B. Royall, E. Clarke, P. Kok, L. R. Wilson, M. S. Skolnick, and A. M. Fox, Nano Lett. **18**, 5475 (2018).
[29] See Supplemental Material at http://link.aps.org/supplemental/10.1103/PhysRevLett.122.173603 for details concerning the sample design, experimental methods and additional results, and input-output modeling of the device, which includes Ref. [30]. We also show that it is possible to control the detuning by Stark shifting the energy of the QD transition.
[30] Ş. E. Kocabaş, E. Rephaeli, and S. Fan, Phys. Rev. A **85**, 023817 (2012).
[31] S. Hughes, Opt. Lett. **29**, 2659 (2004).
[32] V. S. C. Manga Rao and S. Hughes, Phys. Rev. B **75**, 205437 (2007).
[33] M. Arcari, I. Söllner, A. Javadi, S. Lindskov Hansen, S. Mahmoodian, J. Liu, H. Thyrrestrup, E. H. Lee, J. D. Song, S. Stobbe, and P. Lodahl, Phys. Rev. Lett. **113**, 093603 (2014).
[34] D. Hallett, A. P. Foster, D. L. Hurst, B. Royall, P. Kok, E. Clarke, I. E. Itskevich, A. M. Fox, M. S. Skolnick, and L. R. Wilson, Optica **5**, 644 (2018).
[35] J.-T. Shen and S. Fan, Phys. Rev. A **76**, 062709 (2007).
[36] J.-T. Shen and S. Fan, Phys. Rev. Lett. **98**, 153003 (2007).
[37] H. Zheng, D. J. Gauthier, and H. U. Baranger, Phys. Rev. A **82**, 063816 (2010).
[38] S. Xu and S. Fan, Phys. Rev. A **91**, 043845 (2015).
[39] Y. Yu, M. Heuck, H. Hu, W. Xue, C. Peucheret, Y. Chen, L. K. Oxenløwe, K. Yvind, and J. Mørk, Appl. Phys. Lett. **105**, 061117 (2014).
[40] https://doi.org/10.15131/shef.data.7360988.